INSTITUTE OF PHYSICS PUBLISHING JOURNAL OF PHYSICS D: APPLIED PHYSICS
J. Phys. D: Appl. Phys. **38** (2005) 2543–2555 doi:10.1088/0022-3727/38/15/004

Optical properties of human skin, subcutaneous and mucous tissues in the wavelength range from 400 to 2000 nm

A N Bashkatov[1], **E A Genina, V I Kochubey and V V Tuchin**

Institute of Optics and Biophotonics, Saratov State University, 83, Astrakhanskaya Str., Saratov, 410012, Russia

E-mail: bash@optics.sgu.ru

Received 11 January 2005, in final form 7 April 2005
Published 22 July 2005
Online at stacks.iop.org/JPhysD/38/2543

Abstract
The optical properties of human skin, subcutaneous adipose tissue and human mucosa were measured in the wavelength range 400–2000 nm. The measurements were carried out using a commercially available spectrophotometer with an integrating sphere. The inverse adding–doubling method was used to determine the absorption and reduced scattering coefficients from the measurements.

1. Introduction

The development of optical methods in modern medicine in the areas of diagnostics, therapy and surgery has stimulated the investigation of optical properties of various biological tissues, since the efficacy of laser treatment depends on the photon propagation and fluence rate distribution within irradiated tissues. Examples of diagnostic use are the monitoring of blood oxygenation and tissue metabolism [1,2], laser Doppler flowmetry [3], pulse oximetry [4], detection of cancer by fluorescence [5, 6] and spectrophotometric methods [7, 8] and various techniques recently suggested for optical imaging [9–11]. Therapeutic uses include applications in laser surgery [12], laser angioplasty and ablation [13–16] and in photodynamic therapy [17–25]. For these applications, knowledge of tissue optical properties is of great importance for interpretation and quantification of diagnostic data, and for prediction of light distribution and absorbed dose for therapeutic use. The knowledge of tissue optical properties is also necessary for the development of novel optical technologies of photodynamic and photothermal therapy, optical tomography, optical biopsy, etc. Numerous investigations related to determination of tissue optical properties are available. However, the optical properties of many tissues have not been studied in a wide wavelength range.

Review of the literature [5, 6, 17, 19, 21–36] shows that skin and mucous are the most important tissues for photodynamic therapy of cancer and other diseases. Many authors have studied optical properties of these tissues. Recently the skin optical properties have been measured with the integrating sphere technique in the visible and near-infrared (NIR) spectral ranges by Prahl [37], Chan *et al* [38], Simpson *et al* [39], Du *et al* [40] and Troy and Thennadil [41], but the presented data are characteristically different, especially in the IR spectral range. Knowledge of the optical properties of subcutaneous adipose tissue is also important, since optical properties of this tissue layer determine light distribution in the irradiated skin in the course of photodynamic treatment. In addition, analysis of adipose tissue absorption and scattering properties in a wide wavelength range is essential for developing novel optical technologies for treatment of obesity and cellulite, as, evidently, the optical technologies promise less danger to the patient than the widely used surgical and pharmaceutical treatments.

Investigation of the mucous optical properties is necessary for light dosimetry in photodynamic therapy of bladder, colon, oesophagus, stomach, etc. The treatment of purulent maxillary sinusitis is an important problem in modern rhinology, despite the wide application of surgical and pharmaceutical methods [42, 43]. One of the new methods of treatment of this disease is photodynamic therapy of the mucous membrane of the maxillary sinus [42]. The optical properties of mucous tissues were shown by Müller and Roggan [44] for the wavelength 1064 nm. However, in a wide wavelength range the optical properties of mucous tissues have not been studied.

The goal of this paper is to measure the absorption and reduced scattering coefficients of human skin, subcutaneous adipose tissue and mucous in the wavelength range from 400 to 2000 nm.

[1] Author to whom any correspondence should be addressed.

2. Physical properties and structure of the investigated tissues

The skin presents a complex heterogeneous medium, where the blood and pigment content are spatially distributed variably in depth [45–48]. The skin consists of three main visible layers from the surface: epidermis (100 μm thick, the blood-free layer), dermis (1–4 mm thick, vascularized layer) and subcutaneous fat (from 1 to 6 mm thick, in dependence from the body site). Typically, the optical properties of the layers are characterized by the absorption and scattering coefficient, which equals the average number of absorption and scattering events per unit path length of photon travel in the tissue and the anisotropy factor, which represents the average cosine of the scattering angles.

The randomly inhomogeneous distribution of blood and various chromophores and pigments in skin produces variations of the average optical properties of the skin layers. Nonetheless, it is possible to define the regions in the skin, where the gradient of skin cells structure, chromophores or blood amounts, changing with a depth, which roughly equals zero [45]. This allows subdivision of these layers into sublayers, where the physiological nature, physical and optical properties of their cells and pigments content are concerned. The epidermis can be subdivided into two sublayers: non-living and living epidermis. Non-living epidermis or stratum corneum (about 20 μm thick) consists of only dead squamous cells, which are highly keratinized with a high lipid and protein content, and has a relatively low water content [45, 46, 48]. Living epidermis (100 μm thick) contains most of the skin pigmentation, mainly melanin, which is produced in the melanocytes [49]. Large melanin particles such as melanosomes (>300 nm in diameter) exhibit mainly forward scattering. Whereas, melanin dust, whose particles are small (<30 nm in diameter) has the isotropy in the scattering profile and optical properties of the melanin particles (30–300 nm in diameter) may be predicted by the Mie theory.

The dermis is a vascularized layer and the main absorbers in the visible spectral range are the blood haemoglobin, carotene and bilirubin. In the IR spectral range absorption properties of skin dermis are determined by the absorption of water. Following the distribution of blood vessels, [47] skin dermis can be subdivided into four layers: the papillary dermis (150 μm thick), the upper blood net plexus (100 μm thick), the reticular dermis (1–4 mm thick) and the deep blood net plexus (100 μm thick).

The scattering properties of the dermal layers are defined mainly by the fibrous structure of the tissue, where collagen fibrils are packed in collagen bundles and have lamellae structure. The light scatters on both single fibrils and scattering centres, which are formed by the interlacement of the collagen fibrils and bundles. To sum up, the average scattering properties of the skin are defined by the scattering properties of the reticular dermis because of the relatively big thickness of the layer (up to 4 mm [48]) and comparable scattering coefficients of the epidermis and the reticular dermis. Absorption of haemoglobin and water of the skin dermis and lipids of the skin epidermis define absorption properties of the whole skin. It should be noted that absorption of haemoglobin is defined by the haemoglobin oxygen saturation, since absorption coefficients of haemoglobin are different for oxy and deoxy forms. For an adult the arterial oxygen saturation is generally above 95% [4]. Typical venous oxygen saturation is 60–70% [1]. Thus, absorption properties of blood have been defined by absorption of both oxy and deoxy forms of haemoglobin.

The subcutaneous adipose tissue is formed by aggregation of fat cells (adipocytes) containing stored fat (lipids) in the form of a number of small droplets for lean or normal humans and a few or even a single big drop in each cell for obese humans; the lipids are mostly represented by triglycerides [50, 51]. Content of the lipids in a single adipocyte is about 95% of its volume. The diameters of the adipocytes are in the range 15–250 μm [52] and their mean diameter ranges from 50 [50] to 120 μm [51]. In the spaces between the cells there are blood capillaries (arterial and venous plexus), nerves and reticular fibrils connecting each cell and providing metabolic activity to the fat tissue [50, 51]. Absorption of the human adipose tissue is defined by absorption of haemoglobin, lipids and water. The main scatterers of adipose tissue are spherical droplets of lipids, which are uniformly distributed within adipocytes.

The mucous membrane plays a leading role in the physiology of the nose and paranasal sinuses [43, 53]. It is covered with a pseudostratified epithelium, which consists of ciliated, columbar as well as short and long inserted epithelial cells. The membrane called basic divides epithelial and proper layers of the mucous tissue and consists of reticular fibrils, which are located in the interstitial homogeneous media. The membrane does not have a constant thickness. In the case of hyperplasia of the mucous membrane, the membrane thickens considerably [54].

The proper layer of the mucous membrane is similar in structure to connective tissue, consisting of collagen and elastin fibrils. The interstitial fluid of the mucous membrane contains proteins and polysaccharides and is similar in composition to the interstitial fluid of most of the connective tissues. The proper layer of the mucous membrane consists of three sublayers. A subepithelial (or lymphoid) layer contains a great amount of leukocytes. In the intermediate sublayer of the proper layer, tubuloalveolar glands are contained. In the deep sublayer of the proper layer, venous plexuses are arranged, which consist of a surface network of smaller vessels and a deeper network of larger vessels. Normally, the total thickness of the mucous membrane varies from 0.1 to 0.5 mm [43, 53]. In the presence of pathology (maxillary sinusitis, rhinitis or other rhinological disease), the thickness of the mucous membrane increases considerably and can reach 2–3 mm [43]. It should be noted that the proper layer of the mucous membrane is the main layer protecting against micro-organisms causing infectious diseases [53]. The optical properties of the mucous membranes are determined mainly by the optical properties of the proper layer since this layer is much thicker than the epithelial layer.

3. Materials and methods

Measurements have been carried out *in vitro* with skin samples obtained from *post-mortem* examinations and fresh human subcutaneous adipose tissue samples taken from the peritoneum area of patients during planned surgery. Optical

properties of the mucous membrane of the maxillary sinuses were measured for samples, which were obtained from patients with chronic maxillary sinusitis during planned surgery. All tissue samples were kept in saline at room temperature of about 20°C until spectroscopic measurements were carried out. The skin tissue samples were measured one day after autopsy. The adipose tissue samples were measured during 3–4 h after biopsy, and the mucous tissue samples were measured during 2–3 h after biopsy. All the tissue samples were cut into pieces each with an area of about $20 \times 20\,\mathrm{mm}^2$. For mechanical support, the tissue samples were sandwiched between two glass slides. Since compression of tissue causes an increase in the tissue absorption and scattering coefficients [38], in the measurements of the tissue the samples were sandwiched without (or with minimal) compression. In order to provide optical contact between the sample and the glass slides and to prevent the sample compression, the distance between the glass slides was regulated by a special plastic bush, whose thickness varied according to the samples thickness. The thickness of each tissue sample was measured with a micrometer in several points over the sample surface and averaged. Precision of the single measurement was $\pm 50\,\mu$m.

The total transmittance and diffuse reflectance measurements have been performed in the 400–2000 nm wavelength range using the commercially available CARY-2415 ('Varian', Australia) spectrophotometer with an integrating sphere. The inner diameter of the sphere is 100 mm, the size of the entrance port is 20×20 mm and the diameter of the exit port is 16 mm. As a light source, a halogen lamp with filtering of the radiation in the studied spectral range has been used in the measurements. The diameter of incident light beam on the tissue sample is 3 mm. The scan rate is $2\,\mathrm{nm\,s}^{-1}$.

For processing the experimental data and determination of the optical properties of the tissue, the inverse adding–doubling (IAD) method developed by Prahl *et al* [55] has been used. The method is widely used in tissue optics for processing the experimental data of spectrophotometry with integrating spheres [41, 56–60]. This method allows one to determine the absorption (μ_a) and the reduced scattering coefficients ($\mu_s' = \mu_s(1-g)$) of a tissue from the measured values of the total transmittance and the diffuse reflectance. Here μ_s is the scattering coefficient and g is the anisotropy factor of scattering. In these calculations the anisotropy factor has been fixed at 0.9, since this value is typical for many tissues in the visible and NIR spectral ranges [17]. The main advantage of the IAD method, when compared with many other methods of solution of the radiative transfer equation, is related to its validation for the arbitrary ratio of the absorption and scattering coefficients [55]. The property of the IAD method becomes very important in the case of determination of the optical properties of tissues within strong absorption bands, when the values of the absorption and scattering coefficients become comparable. Other methods, such as the diffusion approximation [61–63] or the Kubelka–Munk method [64–66], require, for their applicability, a fulfilment of the condition $\mu_a/\mu_s \ll 1$. The inverse Monte Carlo technique [67] can also be used for the arbitrary ratio of μ_a and μ_s, but requires very extensive calculations. The main limitation of the IAD method is that there may be a possible loss of scattering radiation through the lateral sides of a sample, at calculations [68]. Loss of light through the sides of the sample and the sample holder may erroneously increase the calculated value of the absorption coefficient. These losses depend on the physical size and geometry of the sample, i.e. the losses existing in the case when the sizes of a sample do not significantly exceed the diameter of the incident beam. The size of the exit and the entrance ports of the integrating sphere are also important for errorless measurements of the total transmittance and diffuse reflectance [68]. The tissue sample should completely cover the port in the integrating sphere, and the distance from the edge of the irradiating beam on the sample to the edge of the port should be much larger than the lateral light propagation distance, which is determined by $1/(\mu_a + \mu_s')$. If this is not satisfied, then light will be lost from the sides of the sample and the loss will be attributed to absorption, and so the absorption coefficient will be overestimated. These requirements have been met in our experiments, since maximal size of the sphere port does not exceed 20 mm, whereas the minimal size of the tissue samples is 20 mm. In addition, using the absorption and the reduced scattering coefficients of the investigated tissues presented below, in the next section, we calculated the lateral light propagation distance. For the skin, the maximal lateral light propagation distance is equal to 0.7 mm for the wavelength 1929 nm. For the subcutaneous adipose tissue the maximal value of the lateral light propagation distance is equal to 1.25 mm for the wavelength 1620 nm. For the mucous tissue, the value is equal to 2.2 mm for the wavelength 1284 nm. Taking into account the diameter of the incident beam (3 mm), the minimal size of a tissue sample has to be larger than 7.5 mm, which was satisfied for each tissue sample under study. It is seen that the lateral light propagation distance is smaller than the distance from the edge of the irradiating beam on the sample to the sample port edge. In addition, Pickering *et al* [68] reported that the area of tissue sample has to be smaller than the area of the inner surface of the integrating sphere. This requirement has also been met in our experiments, since the area of the inner surface of integrating sphere used in the measurements was $314.16\,\mathrm{cm}^2$, whereas the area of any tissue sample did not exceed $5.0\,\mathrm{cm}^2$. Figure 1 shows geometry and parameters of the measurements in the transmittance and reflectance modes, respectively.

Calculation of tissue optical properties was performed for each wavelength point. The algorithm consists of the following steps: (a) estimation of a set of optical properties; (b) calculation of the reflectance and transmittance with the adding–doubling iterative method; (c) comparison of the calculated with the measured values of the reflectance and the transmittance; (d) iteration of the above steps until a match (within the specified acceptance margin) is reached. With this iterative process the set of optical properties that yields the closest match to the measured values of reflectance and transmittance are taken as the optical properties of the tissue.

For estimation of the mean size of scatterers of the investigated tissues, the spectroturbidimetric method described in [69] has been used. This method is based on approximation of the scattering coefficient μ_s of turbid media by a power law $\mu_s = a\lambda^{-w}$, where parameter a is defined by the concentration of particles in the media. The wavelength exponent w is independent of the particle concentration and characterizes the

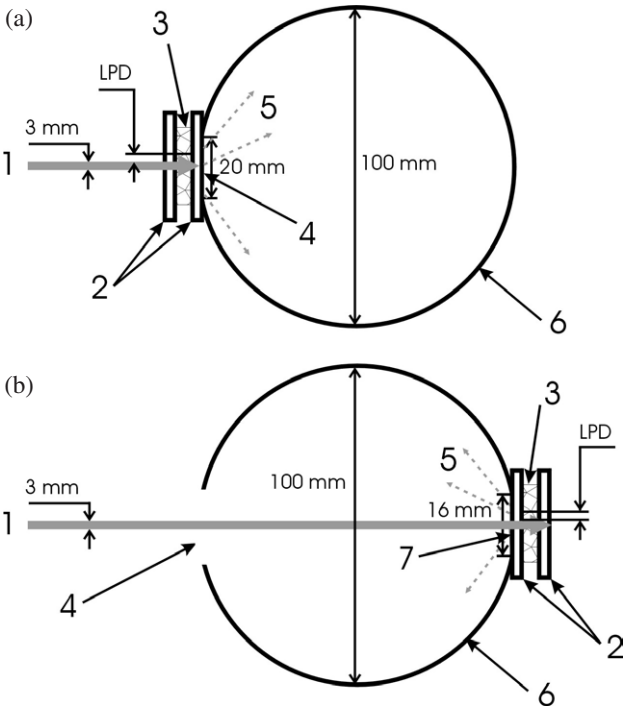

Figure 1. The geometry of the measurements in (*a*) transmittance mode (*b*) reflectance mode. 1—the incident beam (diameter 3 mm); 2—the glass slides; 3—the tissue sample; 4—the entrance port (square 20 × 20 mm); 5—the transmitted (or diffuse reflected) radiation; 6—the integrating sphere (inner diameter is 100 mm); 7—the exit port (diameter 16 mm). LPD—the maximal value of lateral light propagation distance (0.7 mm for skin, 1.25 mm for subcutaneous adipose tissue and 2.2 mm for mucous tissue under study).

mean size of the particles and defines the spectral behaviour of the scattering coefficient [69]. Both the parameter a and the wavelength exponent w are defined by the ratio of refractive indices of the scatterers and environment medium [69]. In experiments, w is expressed in terms of the scattering coefficients measured in a small enough spectral interval (about 200 nm) by the relationship $w = -\partial \ln \mu_s / \partial \ln \lambda$. The substitution in the relationship of a theoretical expression for μ_s obtained for some disperse system models results in equations for determination of either the particle size or the particle refractive index [69]. In the first case, the particle refractive index has to be determined beforehand in independent experiments or has to be obtained from the literature. As a first approximation, w can be calibrated by the formula

$$w(x, m) = \frac{\partial \ln Q(x, m)}{\partial \ln x} \tag{1}$$

with the scattering efficiency factor $Q(x, m)$ calculated for monodisperse system of homogeneous spherical (or cylindrical) isotropic particles. Note that the scattering coefficient μ_s can be connected with the scattering efficiency factor $Q(x, m)$ by the relationship $\mu_s(x, m) = N(\pi d^2/4)Q(x, m)$. Here $m = n_s/n_I$ is the relative refractive index of the scattering particles, i.e. the ratio of the refractive indices of the scatterers (n_s) and the ground materials (i.e. interstitial fluid) (n_I) and x is the dimensionless relative size of scatterers, which is determined as $x = \pi d n_I/\lambda$, where λ is the wavelength, d the diameter of the particles and N the number of scattering particles in the unit of volume.

In the case of spectrophotometric measurements with integrating sphere technique, measured parameter is the reduced scattering coefficient and wavelength dependence of the reduced scattering coefficient can be approximated in accordance with a power law [69–72]

$$\mu_s'(\lambda) = a\lambda^{-w}. \tag{2}$$

On the other hand, the reduced scattering coefficient can be calculated for monodisperse system of spherical particles with the formula $\mu_s'(x, m) = N(\pi d^2/4)Q'(x, m)$, where $Q'(x, m) = Q(x, m)(1 - g)$.

In this case equation (1) can be rewritten in the form

$$w(x, m) = \frac{\partial \ln Q'(x, m)}{\partial \ln x}. \tag{3}$$

In this study, calculation of the scattering efficiency factor $Q(x, m)$ and anisotropy factor g has been performed in accordance with the Mie scattering model, using the algorithm presented by Bohren and Huffman [73].

The mean diameter of the scattering particles has been obtained by minimization of the target function

$$F(x) = (w(x, m) - w^{\exp})^2 \tag{4}$$

with the boundary condition $0.7 \leqslant g \leqslant 0.95$. Here $w(x, m)$ is the wavelength exponent calculated with equation (3) and $w^{\exp}$ is the experimentally measured wavelength exponent value from equation (2). When parameter x was estimated then the mean diameter of the scattering particles was calculated from the relation $d = x\lambda/(\pi n_I)$. In this calculation the refractive indices n_s and n_I for corresponding wavelengths have been obtained from literature.

To minimize the target function, the Levenberg–Marquardt nonlinear least-squares-fitting algorithm, described in detail by Press *et al* [74], has been used. Iteration procedure is repeated until the experimental and the calculated data are matched. As a termination condition of the iteration process, we have used the expression $|w(x, m) - w^{\exp}|/w^{\exp} \leqslant 0.01$.

4. Results and discussion

4.1. Skin optical properties

Twenty-one skin samples obtained from post-mortem examinations were used for the *in vitro* measurements. Figures 2(*a*) and (*b*) and 3(*a*) and (*b*) show the measured optical properties of the human skin samples calculated by the IAD method on the basis of measured values of the total transmittance and the diffuse reflectance. Figure 2(*a*) presents the wavelength dependence of the skin absorption coefficient. The vertical lines correspond to the values of standard deviation (SD), which is determined by $\mathrm{SD} = \sqrt{\sum_{i=1}^{N}(\bar{\mu}_a - \mu_{ai})^2/n(n-1)}$, where $n = 21$ is the number of the measured tissue samples, μ_{ai} is the absorption coefficient of each sample and $\bar{\mu}_a$ is the mean value of the absorption coefficient for each wavelength, which is calculated as $\sum_{i=1}^{N} \mu_{ai}/n$. In the visible spectral range of the spectrum,

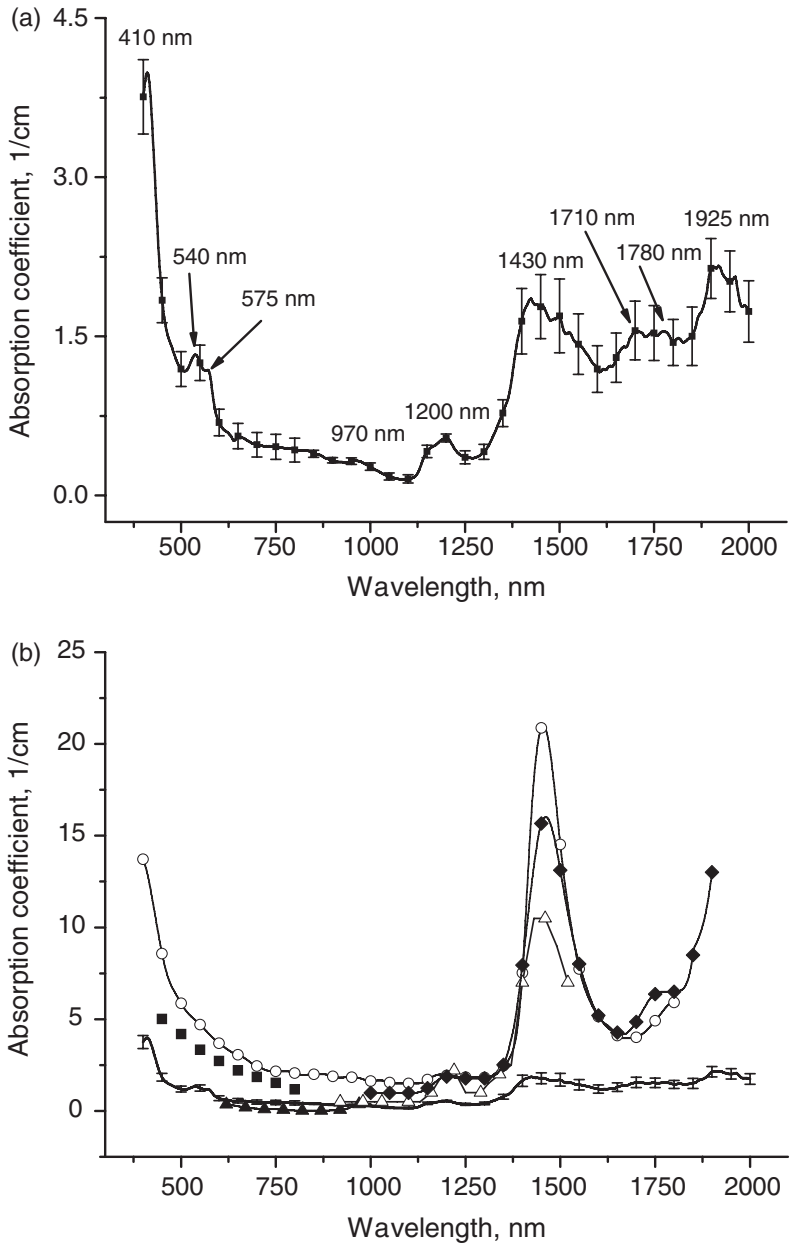

Figure 2. The wavelength dependence of the absorption coefficient μ_a of human skin *in vitro*. (*a*) The vertical lines show the SD values; (*b*) the solid line corresponds to the averaged experimental data and the vertical lines show the SD values. The symbols correspond to the experimental data presented in [37–41]. The squares correspond to the data of [37], the open circles correspond to the data of [38], the up triangles correspond to the data of [39], the open up triangles correspond to the data of [40] and the diamonds correspond to the data of [41].

the absorption bands of oxyhaemoglobin with maximums at 410, 540 and 575 nm are observed [75]. Absorption of water in this spectral range is negligible [76]. In the NIR spectral range, the main chromophores are the water of skin dermis and the lipids of epidermis. In this spectral range the absorption bands of water with maximums at 970 nm [77], 1430 and 1925 nm [78, 79] and lipids with maximums at 1710 and 1780 nm [80] are well seen. At the same time, low-intensity lipid absorption band with the maximum at 930 nm [77] are not observed. Absorption band with the maximum at 1200 nm is the combination of the absorption bands of water (with the maximum at 1197 nm [78, 79]) and lipids (with the maximum at 1212 nm [81]). Increasing the SD in the range of the absorption bands is connected to the differences in the blood and water content in respect of different skin samples. Figure 2(*b*) shows skin absorption coefficient values obtained in this paper (solid line) and those presented by other authors [37–41] (symbols). Comparison of the data obtained in this study and those presented by Simpson *et al* [39] shows an agreement between them. Simpson *et al* [39] reported that in the spectral range 620–1000 nm, skin absorption coefficient is $0.13 \pm 0.12\,\mathrm{cm}^{-1}$. In this spectral range, we obtained $\mu_a \approx 0.37 \pm 0.12\,\mathrm{cm}^{-1}$. Our data are also close to the data of Du *et al* [40] ($\mu_a \approx 0.5 \pm 0.1\,\mathrm{cm}^{-1}$) in the spectral range 900–1100 nm. On the other hand, in this spectral range, Chan *et al* [38] obtained $\mu_a \approx 2.1 \pm 0.5\,\mathrm{cm}^{-1}$. Prahl [37], in the spectral range 620–800 nm obtained, $\mu_a \approx 1.8 \pm 0.4\,\mathrm{cm}^{-1}$. Figure 2(*b*) shows that Chan *et al* [38] (in the spectral range

DOCKET ALARM

Explore Litigation Insights

Docket Alarm provides insights to develop a more informed litigation strategy and the peace of mind of knowing you're on top of things.

Real-Time Litigation Alerts

Keep your litigation team up-to-date with **real-time alerts** and advanced team management tools built for the enterprise, all while greatly reducing PACER spend.

Our comprehensive service means we can handle Federal, State, and Administrative courts across the country.

Advanced Docket Research

With over 230 million records, Docket Alarm's cloud-native docket research platform finds what other services can't. Coverage includes Federal, State, plus PTAB, TTAB, ITC and NLRB decisions, all in one place.

Identify arguments that have been successful in the past with full text, pinpoint searching. Link to case law cited within any court document via Fastcase.

Analytics At Your Fingertips

Learn what happened the last time a particular judge, opposing counsel or company faced cases similar to yours.

Advanced out-of-the-box PTAB and TTAB analytics are always at your fingertips.

API

Docket Alarm offers a powerful API (application programming interface) to developers that want to integrate case filings into their apps.

LAW FIRMS
Build custom dashboards for your attorneys and clients with live data direct from the court.

Automate many repetitive legal tasks like conflict checks, document management, and marketing.

FINANCIAL INSTITUTIONS
Litigation and bankruptcy checks for companies and debtors.

E-DISCOVERY AND LEGAL VENDORS
Sync your system to PACER to automate legal marketing.